Ocean heat uptake efficiency increase since 1970

B. B. Cael[1]

[1]National Oceanography Centre, Southampton, UK.

Key Points:

- Ocean heat uptake has increased from 0.55±0.06 to 0.7±0.02 W/m^{2}K since 1970

Corresponding author: B. B. Cael, `cael@noc.ac.uk`

Abstract

The ocean stores the bulk of excess anthropogenic heat in the Earth system. The ocean heat uptake efficiency (OHUE) – the flux of heat into the ocean per degree of global warming – is therefore a key factor in how much warming will occur in the coming decades. In climate models, OHUE is well-characterised, tending to decrease on centennial timescales; in contrast, OHUE is not well-constrained from Earth observations. Here OHUE and its rate of change are diagnosed from global temperature and ocean heat content records. OHUE increased from $0.57\pm0.06 \mathrm{W/m^2K}$ to $0.7\pm0.02 \mathrm{W/m^2K}$ over the past five decades. This increase is attributed to steepening heat content gradients in the ocean, and corresponds to $\sim$4 years' delay until temperature targets such as 1.5°C or 2°C are exceeded.

Plain Language Summary

Human activity causes extra energy to be radiated to Earth's surface. Much of this extra energy accumulates in the ocean as heat. Based on records of global warming and the ocean's heat content over the past 50 years, here it is shown that the *efficiency* of the transfer of this energy into the ocean has increased in recent decades. This 'ocean heat uptake efficiency' is the amount of energy transferred into the ocean per degree of global warming, and has increased by about 25% from 1970-2021. This translates roughly into a few years' delay until global warming temperature targets, such as 2°C warming, are exceeded.

1 Introduction

Global warming can be understood in terms of conservation of energy of the Earth's surface. The amount of warming corresponds to the difference between the extra energy radiated to the Earth's surface via anthropogenic and natural factors, i.e. the radiative forcing, versus the amount of that energy that is exported elsewhere (Sellers, 1969). A key reservoir for the export of this excess energy is the ocean, which contains almost all of the anthropogenic excess heat in the Earth system (Cheng et al., 2017; Levitus et al., 2012; Domingues et al., 2008; JMA, 2022; Cheng, 2022; JMA, 2022). This ocean heat content (OHC $\mathcal{H}$, [ZJ]) has increased by hundreds of zetajoules over the past several decades of sustained ocean observations (Figure 1), during which time Earth's global mean surface temperature anomaly (T, [K]) has increased by about 1°C (Figure 1) (Morice et al., 2021; Hersbach et al., 2020; Rohde & Hausfather, 2020; Cowtan & Way, 2014; Hansen et al., 2006; Lindsey & Dahlman, 2020).

More important than OHC for future climate change is the ocean heat uptake *efficiency* (OHUE, κ [$\mathrm{W/m^2K}$], Materials and Methods (MM)) (Gregory & Mitchell, 1997; Newsom et al., 2020), that is, how much energy Earth's surface exports downwards into the ocean per degree of global warming. The impact of OHUE on global warming is most simply expressed via a metric referred to as the transient climate sensitivity (TCS [K], MM) (Padilla et al., 2011; Winton et al., 2010; Raper et al., 2002), which expresses the expected warming at the time that the atmospheric CO_2 concentration reaches double its preindustrial level after decades of sustained anthropogenic emissions. TCS is defined as $\mathrm{TCS} = F_{2xCO2}/(\lambda+\kappa)$, where F_{2xCO2} [$\mathrm{W/m^2}$] is the radiative forcing associated with a doubling of the atmospheric CO_2 concentration from preindustrial levels and λ [$\mathrm{W/m^2K}$] is the climate feedback, which analogous to κ corresponds to how much energy Earth's surface exports upwards to space per degree of global warming (Sherwood et al., 2020). The larger the value of κ, the less warming is expected in coming decades.

OHUE is fairly well-characterised within Earth System Models (ESMs). This is mostly via experiments where atmospheric CO_2 is increased by 1% per year for 70 years, after which time it has doubled; OHUE can then be defined as the ratio of $\mathcal{H}$ and T after about 70 years, for instance (Gregory & Mitchell, 1997; Kuhlbrodt & Gregory, 2012). Notably,

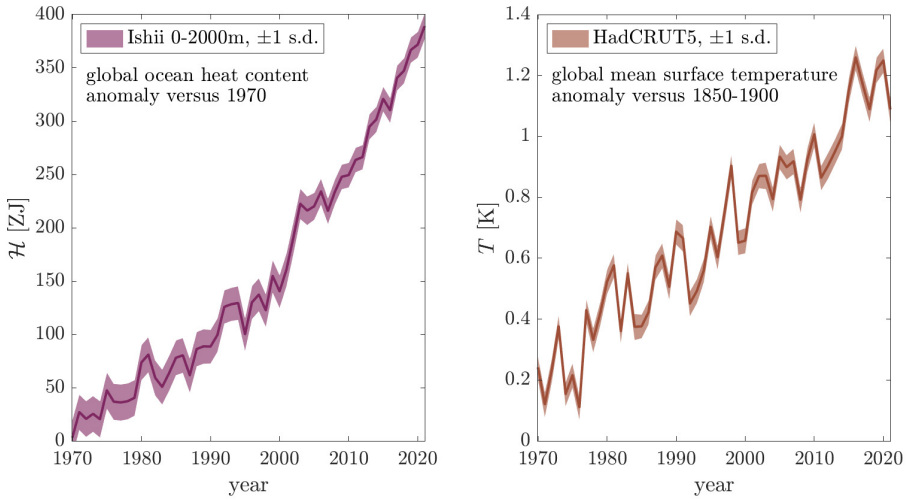

Figure 1. Left: Ocean heat content from (Ishii et al., 2017). Right: Global mean surface temperature from (Morice et al., 2021).

when these experiments are run for 140 years to the point that that atmospheric CO_2 quadruples, OHUE almost always decreases between ∼70 and ∼140 years (Gregory et al., 2015; Watanabe et al., 2013).

In contrast, OHUE is poorly constrained for the real climate system, hindering efforts to validate ESMs' predictions of climate change in coming decades. Here a method is presented to diagnose OHUE from observations of ocean heat content and temperature alone (MM). OHUE has increased from 0.57±0.06 W/m^{2}K to 0.70±0.02 W/m^{2}K over the past five decades. This is attributed to the steepening of heat content gradients in the ocean, rather than ocean circulation changes, and corresponds to a few years' delay in when the temperature targets laid out in the Paris Agreement are exceeded (*Adoption of the Paris Agreement FCCC/CP/2015/L.9/Rev.1*, 2015).

2 Results and Discussion

The method is described in detail in MM. Briefly, the OHC ($\mathcal{H}$) is regressed against the integral of the time-integrated temperature anomaly $\mathcal{T}$; the slope of this regression corresponds to κ. The Ishii (JMA, 2022; Ishii et al., 2017) $\mathcal{H}$ and HadCRUT5 (Morice et al., 2021) T products are used as the uncertainties in these capture uncertainty across other products for these records (MM) (Cheng et al., 2017; Cheng, 2022; Domingues et al., 2008; Levitus et al., 2012; Hersbach et al., 2020; Rohde & Hausfather, 2020; Cowtan & Way, 2014; Hansen et al., 2006; Lindsey & Dahlman, 2020); the years 1970-2021 are used because these are the years with enough signal relative to measurement uncertainties (MM). There is significant curvature in the residuals of this regression (MM), indicating a time-evolution of κ. This is captured by an ansatz that κ changes linearly with time, from an initial value κ_{1970} [W/m^{2}K], by a fixed amount $\delta\kappa_{1970}$ [W/m^{2}K] each year. This ansatz is introduced by replacing $\mathcal{T}$ with a weighted time-integrated temperaturare anomaly $\mathcal{T}_\delta$; the best-fitting δ value for each temperature ensemble member is selected with its corresponding κ_{1970} to quantify uncertainty. The ansatz is then verified by the absence of curvature in the residuals of $\mathcal{H}$ regressed against $\mathcal{T}_\delta$ (Figure 2). Thus, both the time-mean OHUE from 1970-2021 and the time evolution of OHUE, as approximated by a linear trend, are captured.

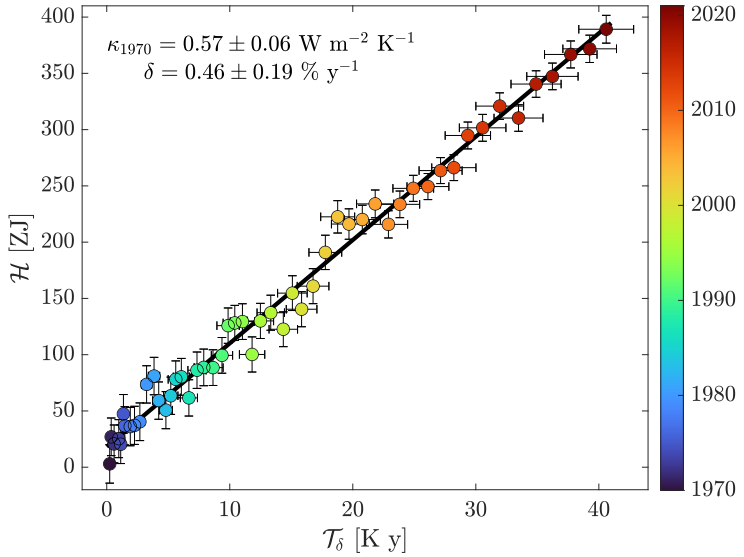

Figure 2. Regression of ocean heat content vs. weighted temperature integral to find initial ocean heat uptake efficiency and rate of change.

Figure 3 shows the joint distribution of the initial OHUE, i.e. κ_{1970}, and the fractional annual change relative to this initial value (δ). It is found with 99% probability that OHUE increased (i.e. $\delta > 0$) from 1970-2021, and that this increase is well-described as linearly increasing with time rather than being a temperature-dependent effect or having higher-order time-dependence (MM). The uncertainty in these two parameters is highly anticorrelated, such that the time-mean OHUE from 1970-2021, 0.63±0.04 W/m^{2}K, has reduced uncertainty relative to that of $\kappa_{1970} = 0.57 \pm 0.06$ W/m^{2}K. This trend corresponds to a fairly large relative change of 24±10% in OHUE over the past five decades, with a value in 2021 of 0.7±0.02 W/m^{2}K (Figure 4). This linear trend corresponds to an additional 66 ± 20 ZJ of heat stored in the ocean during this time period versus if OHUE stayed at its 1970 value (κ_{1970}) over 1970-2021, which is enough to heat the top ∼25m of the ocean by 1°C, and 17±5% of the total OHC accumulated during this time period. This linear trend also has appreciable consequences for near-term warming. Using standard values of $F_{2xCO2} = 4 \pm 0.3$ W/m^2 and $\lambda = 1.3 \pm 0.44$ W/m^{2}K, under a scenario where atmospheric CO_2 increases by 1% a year, a κ like that diagnosed for 1970 results in the exceeding 1.5°C (2°C) warming by 3.5±1.1 years (4.6±1.5 years) earlier than a κ like that diagnosed for 2021. While these calculations are based on the heuristic metric of TCS, they still nonetheless underscore an appreciable evolution of κ diagnosed here in terms of climate policy and projection. This difference will of course be even greater if the increase in κ continues, with opposite implications if the trend reverses in the near future.

The increase in OHUE from 1970-2021 is attributed to the steepening of heat content gradients over this time period as excess heat is accumulated in the ocean. Heat is primarily stored in the ocean in i) the North Atlantic and ii) the Southern Ocean due to the overturning circulation, and iii) via stirring and mixing of gradients by eddies and other forms of ocean turbulence. The increase in OHUE cannot be due to the first two of these, principally because the overturning circulation in neither the North Atlantic nor the Southern Ocean has shown a definite systemic strengthening over this time period (Meredith et al., 2012; Kilbourne et al., 2022). In contrast, the gradients of excess heat in the ocean have steadily increased over this time period as heat is continually in-

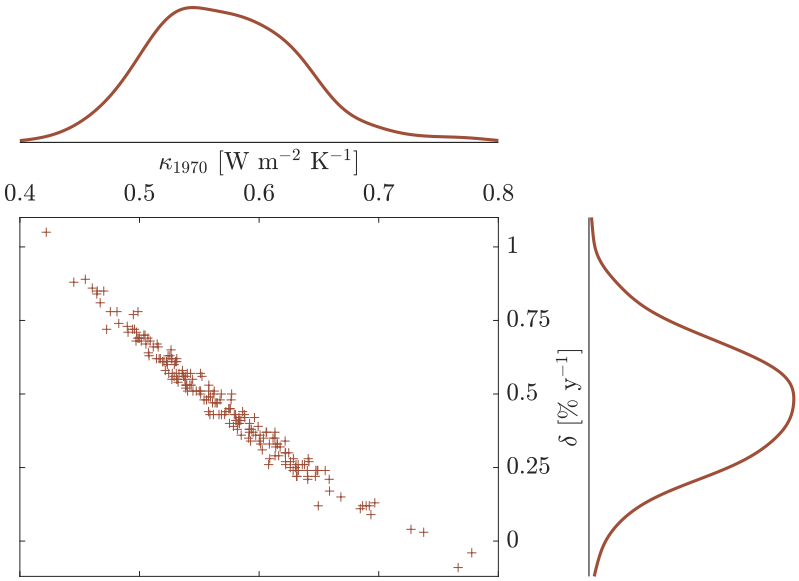

Figure 3. Joint distribution of initial ocean heat uptake efficiency and rate of change.

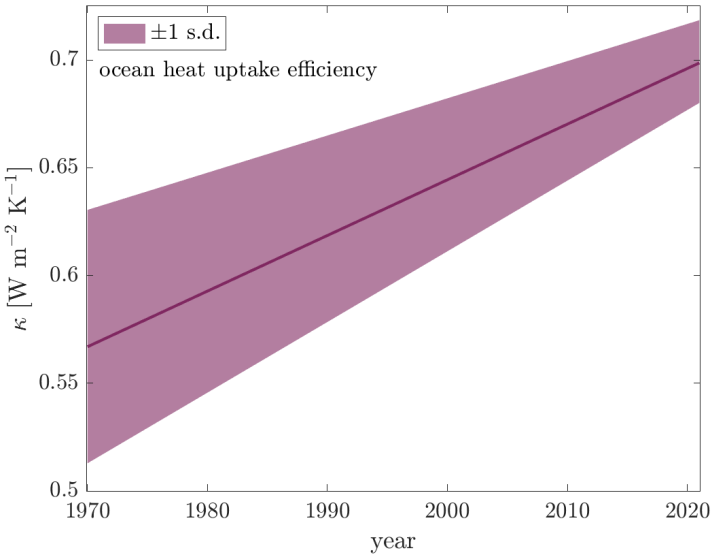

Figure 4. Ocean heat uptake efficiency vs. time.

jected into the upper ocean and comparatively slowly diffused into its interior (Cheng et al., 2017; Cheng, 2022). Analogous to Fick's first law of diffusion, the steeper the gradients of anthropogenic heat, the more efficiently ocean turbulent processes can act to transport heat away from the surface. This results in a larger OHUE, because every additional amount of heat added to the surface ocean can be more easily transported into the ocean interior as these gradients steepen. This is also visible in the increased fraction of total OHC contained in deeper layers of the ocean over time (Cheng et al., 2017; Cheng, 2022). The change in κ is thus a result of passive transport of heat by ocean dynamics, rather than by the direct influence of the injected heat on the ocean's dynamics. This also explains why the change in κ is better explained as a temporal evolution than a temperature-dependent climate feedback, as its change is due to the steady steepening of these gradients.

As this is a generic phenomenon, the increase in OHUE over time is expected to continue in the near future, as anthropogenic heat gradients should continue to steepen in the ocean. Note that no evidence for a reversal of this increasing trend is observable in the residuals of the regression in Figure 2. However, this multidecadal increase in κ is not necessarily in disagreement with the centennial-scale decrease in κ observed in ESMs, which is thought to be due to the equilibration of the deep ocean with Earth's surface, i.e. the eventual smoothing out of anthropogenic heat gradients (Gregory et al., 2015; Watanabe et al., 2013). Even under sustained radiative forcing, the deep ocean should eventually accumulate enough heat to weaken these heat gradients and OHUE should therefore decrease, as found in ESM experiments. ESMs should however be able to replicate this multidecadal increase in κ, though they are expected to reach an equilibrium temperature (corresponding to the equilibrium climate sensitivity) at some point after radiative forcing is stabilised. It is possible however that 140 years is too fast a timescale to expect the deep ocean to equilibrate with Earth's surface under sustained emissions. It would be instructive to investigate the centennial κ behaviour within ESMs that can resolve the multidecadal increasing trend in κ diagnosed from observations here. OHUE may also decrease over time due to overturning circulation changes that have not yet occurred. Altogether these results demonstrate the importance of deriving observational estimates of the key climate parameters that determine the Earth's response to anthropogenic forcing, as well as the evolution of these parameters over time, as critical counterpoints to ESM estimates both to evaluate models and to make independent projections.

3 Materials and Methods

Theory: The flux of energy from the Earth's surface boundary layer into the ocean H [ZJ/year] can be integrated from an initial time point t_i to yield the ocean heat content anomaly $\mathcal{H}(t)$ [ZJ]:

$$\mathcal{H}(t) = \int_{t_i}^{t} H(\tau)\ d\tau$$

where τ is a dummy variable. The ocean heat content efficiency κ [ZJ/K y] is defined as this energy flux per degree of global warming, i.e. $\kappa = H/T$ so that

$$\mathcal{H}(t) = \int_{t_i}^{t} H(\tau)\ d\tau = \int_{t_i}^{t} \kappa(\tau)T(\tau)\ d\tau$$

The ansatz is then made that $\kappa = \kappa_i(1 + \delta(t - t_i))$, i.e. κ starts at κ_i at t_i and increases by a constant amount $\delta\kappa_i$ each year – δ here is a number (in units of y^{-1}), not the Kronecker delta function. For simplicity t_i is redefined as year zero so $\kappa = \kappa_i(1 + \delta t)$; one can then substitute

$$\mathcal{H}(t) = \int_{t_i}^{t} \kappa_i(1+\delta\tau)T(\tau)\ d\tau = \kappa_i \int_{t_i}^{t} (1+\delta\tau)T(\tau)\ d\tau$$

The year 1970 is then redefined as the initial year and the initial ocean heat uptake efficiency is labeled as κ_{1970} for clarity. If one then defines

$$\mathcal{T}_\delta(t) = \int_{t_i}^{t} (1+\delta\tau)T(\tau)\ d\tau$$

then the slope

$$\mathcal{H}(t)/\mathcal{T}_\delta(t) = \kappa_{1970}$$

If the ansatz is valid and the correct δ is selected, this δ will capture all the time-dependence of κ and this slope will be constant in time, i.e. there will be no systematic behavior or curvature in the residuals of $\mathcal{H}(t)$ regressed against $\mathcal{T}_\delta(t)$. Finally for Figures 2-4, κ is divided by a factor of 16.09 to convert zetajoules per degree Kelvin per year to watts per square meter per second; note that this is an average over the full Earth surface, not just the ocean surface, in keeping with the standard definition.

Temperature data: The HadCRUT5 temperature record is used here, which is provided as a 200-member ensemble. HadCRUT5 is described in detail in (Morice et al., 2021). $T(t)$ [K] is defined as the temperature anomaly versus the 1850-1900 average. This temperature record is selected because i) uncertainties being expressed as ensemble members makes the propagation of uncertainty straightforward when integrating in time, and ii) the HadCRUT5 ensemble captures the uncertainty across temperature time series. Specifically, when 0.03 K is subtracted from the $T(t)$ ensemble, 99% of the temperatures across all years of five other temperature products (Hersbach et al., 2020; Rohde & Hausfather, 2020; Cowtan & Way, 2014; Hansen et al., 2006; Lindsey & Dahlman, 2020) are above (below) the 1st (99th) percentile of the ensemble. This value of 0.03 K is subtracted from the ensemble for the calculations herein, but this does not change the results.

Ocean heat content data: The Ishii ocean heat content record is used here, which is provided as a mean ocean heat content over 0-2000m, with associated time-varying Gaussian uncertainty. The Ishii time series is described in detail in (Ishii et al., 2017). $\mathcal{H}(t)$ [ZJ] is defined as the ocean heat content anomaly versus 1970. This ocean heat content record is selected because i) uncertainties are explicitly calculated for 0-2000m, rather than separately for 0-700m and 700-2000m with unspecified uncertainty correlation, and ii) the Ishii time series captures the uncertainty across ocean heat content time series. Specifically, when 3 ZJ is added to the $\mathcal{H}(t)$ ensemble, 99% of the ocean heat content values across all years of two other observational products (Cheng et al., 2017; Domingues et al., 2008; Levitus et al., 2012; Cheng, 2022) are above (below) the 1% (99%) confidence level of the time series. Reanalysis products are not considered because these "are not suitable for studies of long-term trends or low frequency variability across data-sparse time periods" (Killick & for Atmospheric Research Staff (Eds.), 12 June 2020). This value of 3 ZJ is added to the $\mathcal{H}(t)$ time series for the calculations herein, but this does not change the results. Years 1970 onwards are considered because i) ocean heat content changes are more sparsely observed and uncertain before this year, ii) changes in both ocean heat content and temperature are very small over the years that ocean heat content data are available prior to this year compared to both this uncertainty and interannual variability, indicating there is little to no signal to extract, and iii) 1970 is the first year for which multiple other observational ocean heat content products are available for comparison

to verify that the Ishii ocean heat content uncertainties encapsulate across-product uncertainty in ocean heat content.

Initial curvature calculation: Time-evolution of κ (i.e. $\delta \neq 0$) is tested for initially by regressing $\mathcal{H}(t)$ versus each ensemble member of $\mathcal{T}_{\delta=0}(t)$. A weighted quadratic regression is performed, with weights equal to the inverse square of the 1σ uncertainty in $\mathcal{H}$. For all of these regressions the quadratic term is positive, indicating that δ is significantly positive and necessary to describe the relationship between T and $\mathcal{H}$.

Primary analysis: To generate an estimate of κ_{1970} and δ, for each $T(t)$ ensemble member, the following procedure is followed: i) sample a large range of δ values (in practice the range -0.002 to 0.011 at 0.0001 resolution is sufficient; see Fig. 3), ii) calculate $\mathcal{T}_\delta(t)$ for each, iii) perform a linear, quadratic, and cubic weighted regression of $\mathcal{H}(t)$ against $\mathcal{T}_\delta(t)$ for each, iv) discard any δ values for which the quadratic and/or cubic coefficients are significantly different from zero (at the 5% confidence level, but using 10% or 1% confidence levels made no difference to the results) as these indicate curvature remains in the residuals and therefore δ does not capture the time-evolution of κ in the data, v) select the δ value for which the linear regression has the lowest residual sum of squares (or equivalently the highest r^2 or equivalently the lowest root-mean-square error). The associated κ_{1970} is the slope of this δ's linear regression (Fig. 2). These δ values yielded highly linear relationships between $\mathcal{H}(t)$ and $\mathcal{T}_\delta(t)$; the quadratic terms are 0.18±0.05 (max. 0.31) z-scores away from zero, while the cubic terms are 0.27±0.10 (max. 0.55) z-scores away from zero.

Temperature vs. time analysis: The evolution of κ as a function of time is compared to that of a temperature-dependent κ, i.e. the ansatz $\kappa = \kappa_{1970}(1+\delta T)$ is compared to the ansatz $\kappa = \kappa_{1970}(1 + \delta t)$ in the main text. A temperature-dependent κ would correspond to a type of temperature-dependent climate feedback, whereby the climate sensitivity depends on the temperature itself (Bloch-Johnson et al., 2021). The above analysis is repeated with the alternative ansatz to evaluate which model has the lower residual sum of squares (or equivalently the higher r^2 or equivalently the lower root-mean-square error); in 98.5% (197/200) instances this is the time-dependent model, indicating the ansatz in the text is a better description of the evolution of κ than a temperature-dependent κ.

Years to 1.5 or 2°C: To estimate the difference in years taken to surpass 1.5°C or 2°C,the transient climate sensitivity $TCS = F_{2\times CO_2}/(\lambda + \kappa)$ is calculated, where $F_{2\times CO_2} \sim N(4.0, 0.3)$ W/m^2 is the radiative forcing associated with a doubling of CO_2 and $\lambda \sim N(1.3, 0.44)$ W/m^{2}K is the climate feedback (Sherwood et al., 2020). Note that the TCS is closely related to the arguably more relevant metric of the transient climate response (Winton et al., 2010); the TCS is preferred in this context, however, as the TCR would require a specification of the surface boundary layer's heat capacity, a term that is less certain than those that comprise the TCS. The TCS analysis is equivalent to TCR under the plausible assumption that the surface boundary layer's heat capacity is on the order of 30 ZJ or less, equivalent to roughly the top 10m of the global ocean. The year of crossing a temperature threshold of C degrees is then defined as $y = 70C/TCS$; 70 is the number of years that is required for atmospheric CO_2 concentrations to increase at 1% per year until the concentration doubles, which corresponds to a linear increase in radiative forcing under the assumption of logarithmic CO_2 forcing (Bloch-Johnson et al., 2021). For each (κ_{1970}, δ) pair, a random value of $F_{2\times CO_2}$ and λ are sampled from the distributions above, and y is calculated for $C = 1.5$ and 2°C, and for κ_{1970} and $\kappa_{2021} = \kappa_{1970}(1 + 51\delta)$. The difference $y(C = 2, \kappa_{2021}) - y(C = 2, \kappa_{1970})$ is 4.6±1.5 years; the difference $y(C = 1.5, \kappa_{2021}) - y(C = 1.5, \kappa_{1970})$ is 3.5±1.1 years. Note that this is a heuristic metric and is only intended to illustrate the potential impact of the change in κ diagnosed herein.(Morice et al., 2021)

Acknowledgments

It is a pleasure to thank the many scientists whose collective work has generated the time series on which this work relies. This work was support by the European Union's Horizon 2020 Research and Innovation Programme under grant agreement No. 820989 (project COMFORT). The work reflects only the authors' view; the European Commission and their executive agency are not responsible for any use that may be made of the information the work contains. Cael conceived the study, performed the analyses, and wrote the paper. The author has no competing interests to declare. **Open Research:** The data on which this article is based are available in (JMA, 2022; Ishii et al., 2017) and (Morice et al., 2021; MetOffice, 2022). Code is available for review purposes at github.com/bbcael/ohue and will be deposited to a FAIR compliant repository if this article is eventually accepted.

References

Adoption of the Paris Agreement FCCC/CP/2015/L.9/Rev.1. (2015). UNFCCC.

Bloch-Johnson, J., Rugenstein, M., Stolpe, M. B., Rohrschneider, T., Zheng, Y., & Gregory, J. M. (2021). Climate sensitivity increases under higher co2 levels due to feedback temperature dependence. *Geophysical Research Letters*, *48*(4), e2020GL089074.

Cheng, L. (2022). *OHC by IAP.* `http://159.226.119.60/cheng/`. ([Online; accessed 7-April-2022])

Cheng, L., Trenberth, K. E., Fasullo, J., Boyer, T., Abraham, J., & Zhu, J. (2017). Improved estimates of ocean heat content from 1960 to 2015. *Science Advances*, *3*(3), e1601545.

Cowtan, K., & Way, R. G. (2014). Coverage bias in the hadcrut4 temperature series and its impact on recent temperature trends. *Quarterly Journal of the Royal Meteorological Society*, *140*(683), 1935–1944.

Domingues, C. M., Church, J. A., White, N. J., Gleckler, P. J., Wijffels, S. E., Barker, P. M., & Dunn, J. R. (2008). Improved estimates of upper-ocean warming and multi-decadal sea-level rise. *Nature*, *453*(7198), 1090–1093.

Gregory, J. M., Andrews, T., & Good, P. (2015). The inconstancy of the transient climate response parameter under increasing co2. *Philosophical Transactions of the Royal Society A: Mathematical, Physical and Engineering Sciences*, *373*(2054), 20140417.

Gregory, J. M., & Mitchell, J. F. (1997). The climate response to co2 of the hadley centre coupled aogcm with and without flux adjustment. *Geophysical Research Letters*, *24*(15), 1943–1946.

Hansen, J., Ruedy, R., Sato, M., & Lo, K. (2006). Nasa giss surface temperature (gistemp) analysis. *Trends: A Compendium of Data on Global Change*.

Hersbach, H., Bell, B., Berrisford, P., Hirahara, S., Horányi, A., Muñoz-Sabater, J., ... others (2020). The era5 global reanalysis. *Quarterly Journal of the Royal Meteorological Society*, *146*(730), 1999–2049.

Ishii, M., Fukuda, Y., Hirahara, S., Yasui, S., Suzuki, T., & Sato, K. (2017). Accuracy of global upper ocean heat content estimation expected from present observational data sets. *Sola*, *13*, 163–167.

JMA. (2022). *JMA's global ocean heat content data.* `https://www.data.jma.go.jp/gmd/kaiyou/english/ohc/ohc_data_en.html`. ([Online; accessed 7-April-2022])

Kilbourne, K. H., Wanamaker, A. D., Moffa-Sanchez, P., Reynolds, D. J., Amrhein, D. E., Butler, P. G., ... others (2022). Atlantic circulation change still uncertain. *Nature Geoscience*, *15*(3), 165–167.

Killick, R., & for Atmospheric Research Staff (Eds.), N. C. (12 June 2020). *The Climate Data Guide: EN4 subsurface temperature and salinity for the global oceans.* `https://climatedataguide.ucar.edu/climate-data/en4-subsurface-temperature-and-salinity-global-oceans`. ([Online;

accessed 7-April-2022])

Kuhlbrodt, T., & Gregory, J. (2012). Ocean heat uptake and its consequences for the magnitude of sea level rise and climate change. *Geophysical Research Letters*, *39*(18).

Levitus, S., Antonov, J. I., Boyer, T. P., Baranova, O. K., Garcia, H. E., Locarnini, R. A., ... others (2012). World ocean heat content and thermosteric sea level change (0–2000 m), 1955–2010. *Geophysical Research Letters*, *39*(10).

Lindsey, R., & Dahlman, L. (2020). Climate change: Global temperature. *Climate. gov*, *16*.

Meredith, M. P., Naveira Garabato, A. C., Hogg, A. M., & Farneti, R. (2012). Sensitivity of the overturning circulation in the southern ocean to decadal changes in wind forcing. *Journal of Climate*, *25*(1), 99–110.

MetOffice. (2022). *The met office hadley centre observations datasets: Hadcrut5.* `https://www.metoffice.gov.uk/hadobs/hadcrut5/`. ([Online; accessed 7-April-2022])

Morice, C. P., Kennedy, J. J., Rayner, N. A., Winn, J., Hogan, E., Killick, R., ... Simpson, I. (2021). An updated assessment of near-surface temperature change from 1850: The hadcrut5 data set. *Journal of Geophysical Research: Atmospheres*, *126*(3), e2019JD032361.

Newsom, E., Zanna, L., Khatiwala, S., & Gregory, J. M. (2020). The influence of warming patterns on passive ocean heat uptake. *Geophysical Research Letters*, *47*(18), e2020GL088429.

Padilla, L. E., Vallis, G. K., & Rowley, C. W. (2011). Probabilistic estimates of transient climate sensitivity subject to uncertainty in forcing and natural variability. *Journal of Climate*, *24*(21), 5521–5537.

Raper, S. C., Gregory, J. M., & Stouffer, R. J. (2002). The role of climate sensitivity and ocean heat uptake on aogcm transient temperature response. *Journal of Climate*, *15*(1), 124–130.

Rohde, R. A., & Hausfather, Z. (2020). The berkeley earth land/ocean temperature record. *Earth System Science Data*, *12*(4), 3469–3479.

Sellers, W. D. (1969). A global climatic model based on the energy balance of the earth-atmosphere system. *Journal of Applied Meteorology and Climatology*, *8*(3), 392–400.

Sherwood, S., Webb, M. J., Annan, J. D., Armour, K. C., Forster, P. M., Hargreaves, J. C., ... others (2020). An assessment of earth's climate sensitivity using multiple lines of evidence. *Reviews of Geophysics*, *58*(4), e2019RG000678.

Watanabe, M., Kamae, Y., Yoshimori, M., Oka, A., Sato, M., Ishii, M., ... Kimoto, M. (2013). Strengthening of ocean heat uptake efficiency associated with the recent climate hiatus. *Geophysical Research Letters*, *40*(12), 3175–3179.

Winton, M., Takahashi, K., & Held, I. M. (2010). Importance of ocean heat uptake efficacy to transient climate change. *Journal of Climate*, *23*(9), 2333–2344.